

Research Article

Photorealistic Modeling of the Growth of Filamentous Specimens

Jiří Sedlář,^{1,2} Jan Flusser,¹ and Michaela Sedlářová³

¹ Department of Image Processing, Institute of Information Theory and Automation, Academy of Sciences of the Czech Republic, Pod vodárenskou věží 4, 182 08 Prague 8, Czech Republic

² Faculty of Mathematics and Physics, Charles University, Malostranské náměstí 25, 118 00 Prague 1, Czech Republic

³ Department of Botany, Faculty of Science, Palacký University, Šlechtitelů 11, 783 71 Olomouc – Holic, Czech Republic

Correspondence should be addressed to Jiří Sedlář, sedlar@utia.cas.cz

Received 27 April 2007; Revised 8 October 2007; Accepted 14 October 2007

Recommended by Stephen Marshall

We present a new method for modeling the development of settled specimens with filamentous growth patterns, such as fungi and oomycetes. In phytopathology, the growth parameters of such microorganisms are frequently examined. Their development is documented repeatedly, in a defined time sequence, leaving the growth pattern incomplete. This restriction can be overcome by reconstructing the missing images from the images acquired at consecutive observation sessions. Image warping is a convenient tool for such purposes. In the proposed method, the parameters of the geometric transformation are estimated by means of the growth tracking based on the morphological skeleton. The result is a sequence of photorealistic artificial images that show the development of the specimen within the interval between observations.

Copyright © 2008 Jiří Sedlář et al. This is an open access article distributed under the Creative Commons Attribution License, which permits unrestricted use, distribution, and reproduction in any medium, provided the original work is properly cited.

1. INTRODUCTION

In various fields of biology and medicine, the growth parameters of microorganisms are frequently examined. However, the equipment allowing continuous monitoring of specimens over long periods of time is expensive, and sometimes even inconvenient for the purpose of the study. In phytopathology, for example, special conditions for cultivation are often required. Although life-imaging systems equipped with controlled environment parameters have been introduced, such microscopes are adapted for human and animal cells research, that is, with temperature range inappropriate for phytopathogenic fungi. Such specimens have to be cultivated separately, in optimal conditions, and observed repeatedly, in a defined time sequence. In contrast to the monitoring systems, this approach allows examination of multiple samples during each observation session. However, as the acquisition and documentation process is elaborate, the intervals between observations are usually quite long, that is, of several hours in the case of fungal specimens. Sometimes the intervals are so long that the series of acquired images lacks information important for the purpose of the study, as significant changes in the shape of the specimen were not doc-

umented. In order to examine the missing stages of growth and complete the development pattern, a series of images acquired at appropriately short intervals would be necessary. In the case of biomedical samples, however, the experiments cannot be repeated with the same results because every specimen develops in a unique way, and thus additional observations are not feasible. This restriction can be overcome by reconstructing the missing images, representing the specimen in the intervals between acquisitions, from the available ones. We aim to propose such a method in this paper.

Realistic modeling of specimen development over undocumented intervals is quite complex. Although the problem can be described as interpolation over time, the spatial deformations cannot be simulated just by a pixel-wise interpolation of pixel values. In order to generate realistic images, understanding of the growth mechanism is necessary. The model is required to preserve the characteristics of the specimen and to avoid an introduction of significant artificial deformations so that it could be utilized to process biomedical data.

The problem of photorealistic modeling of the growth of biological specimens has not been satisfactorily solved yet. As a general method for arbitrary types of specimens would



FIGURE 1: *Fusarium oxysporum* f.sp. *pisi*. An early (a) and a later (b) image of one specimen from consecutive observation sessions. The development of two hyphae from a macroconidium and their growth in length. Light microscopy images after preprocessing, namely flat-field correction, displacement rectification, multifocal fusion, and debris suppression.

be too complex, we will restrict ourselves to time studies of settled specimens with filamentous growth patterns, such as fungi and oomycetes. Whereas their filaments elongate over time, their growth in width is negligible, and the shape of the already developed parts does not change significantly. Also, each filament develops in its own speed. All these properties will be utilized in the proposed method.

In general, two different approaches to the problem of modeling object development over time exist. One approach is based on mathematical modeling and computer graphics. It constructs a mathematical model of the object according to the acquired images. The changes in geometry are simulated by adjusting the parameters of the model. For the purpose of visualization, standard rendering techniques are employed. L-system grammars [1] have been successfully used for modeling the growth of settled biological specimens such as plants [2] and fungal pathogens [3]. The main drawback of these methods is the artificial appearance of the generated images.

The alternative approach is based on image morphing [4]. It utilizes image warping to geometrically transform the images acquired at the beginning and at the end of the missing interval to represent a particular instance within the interval. These warped images are composed into a single image, in ratio corresponding to the position of the instance within the interval. To visualize the development, a series of such blended images representing instances within the interval is generated. This approach preserves the natural appearance of the original images. Image morphing has been widely used in computer graphics to generate artificial motion sequences [5] or smooth transitions between objects [6], as well as to map image textures onto 3D objects. Image warping is also commonly utilized in image processing to rectify geometric distortions [7].

We introduce a new method for photorealistic modeling of the growth of settled specimens with filamentous growth patterns over intervals between acquisitions. The method is based on growth tracking by means of the morphological skeleton and image warping by means of the radial basis functions. Its performance is demonstrated on real data.

2. METHODS

Our task is to generate photorealistic images representing the growth of a specimen within an interval between observations. We propose to reconstruct them from the available images by means of an appropriate geometric transformation. In order to establish its parameters, we select a sufficient number of control points (CPs) in the images acquired at the beginning and at the end of the examined interval. The CPs should correspond to salient features of the specimen, such as points on its boundary. Then we estimate how their positions were changing over the interval. Finally, we geometrically transform the input images so that the selected CPs are mapped to their estimated positions. As a result, we obtain a sequence of artificial yet photorealistic images showing the specimen development over the undocumented interval.

The trajectory of the CPs cannot be estimated simply by means of a linear interpolation of their positions at the beginning and at the end of the interval. For this purpose, an appropriate growth tracking method must be used. Most object tracking methods, including the commonly used active contours (“snakes”) [8], are based on object boundaries. These techniques, however, do not respect the unisotropic growth pattern of biological specimens. Consequently, they tend to significantly distort the shape of curved boundaries during the interpolation process and the estimated trajectory of the CPs on the boundary is thus inaccurate. The warped images generated using such methods would suffer from unnatural artificial deformations, especially in the case of curved filamentous objects. Such a drawback could lead to false conclusions regarding the biology of the species.

In order to avoid this problem, we propose to utilize the properties of the morphological skeleton (MS), a thin-line representation of an object. In this case, the branches of the MS correspond to the filaments of the specimen. The skeleton is computed from a segmented image by means of appropriate morphological operations. There are many skeletonization algorithms with different results. Most of them are based on thinning [9], a morphological operation that repeatedly erodes object boundary while preserving pixel-wide



FIGURE 2: Binary images of the shape of the specimen in Figure 1. Image segmentation by means of adaptive thresholding.

structures. For the purposes of growth tracking, we propose to compute the MS by an algorithm insensitive to contour noise so that the MS does not contain spurs and distorted line endings.

The MS is less sensitive to curving deformations than the boundary, as the length of the branches is preserved. Hence, we propose to select the CPs equidistantly along the MS of the specimen in the image acquired at the beginning of the missing interval. The changes in their positions are estimated by elongating the branches of this MS along the corresponding branches of the MS in the image acquired at the end of the interval so that the distance between the CPs on each branch remains uniform. This simulates the growth of the specimen in length over the undocumented interval without unnatural deformations of curved filaments.

We make a few assumptions about the pair of MSs from consecutive observation sessions. First, we suppose that the number of segments in both MSs is the same, that is, no new filaments evolve in the interval between acquisitions. We neglect possible short spurs in the second, latter MS that have no counterpart in the first, earlier MS, as they are insignificant in this stage of growth. Then, as we suppose that the already grown parts do not move or develop new bends, the second MS should roughly overlap the whole first MS. Finally, we assume that each branch elongates uniformly over time. In the case of settled specimens with filamentous growth patterns, these assumptions are usually satisfied.

The parameters of the geometric transformation, however, cannot be estimated just by means of the CPs on the MS. The boundary of the specimen is not well defined by such CPs and curved filaments would consequently appear unnaturally deformed in the warped image. Hence, we propose to spread the CPs from the MS to the boundary of the specimen. We replace each CP on the MS (skeleton-CP) by a pair of points on the boundary of the object (boundary-CPs) in the direction perpendicular to the MS. These boundary-CPs are used as control points in image warping. As a result, the appearance of the warped images is very realistic, without significant artificial deformations.

The aim of the geometric transformation is to map the control points from one of the available images to the posi-

tions estimated in the process described above. Due to the spatially local character of the growth process, the transformation should be sensitive to such local changes. Elastic types of geometric transformations, such as radial basis functions (RBF) [10], have been used for such purposes with satisfactory results. The RBFs define a coordinate transformation:

$$f(\mathbf{x}) = p_m(\mathbf{x}) + \sum_{i=1}^n \alpha_i \phi_i(\|\mathbf{x} - \mathbf{x}_i\|), \quad (1)$$

which consists of a linear combination of basis functions ϕ_i centered in control points \mathbf{x}_i . The functions are called radial as the value of each basis function ϕ_i depends only on the distance from its center \mathbf{x}_i . The properties of the transformation f depend on the type of the basis functions ϕ_i used. For our purposes, we propose to use thin-plate splines (TPS):

$$\phi_i(r) = r^2 \log r \quad (2)$$

because of their smooth character. The weights α_i are computed by placing the centers x_i into (1) and solving the resulting set of linear equations. The polynomial term p_m allows a certain degree of polynomial precision so that where the influence of the basis functions ϕ_i tends to zero, the result of the transformation will be dominated by this term. When the images do not exhibit global deformations, it is defined simply as $p_m(\mathbf{x}) = \mathbf{x}$.

3. RESULTS

The performance of the proposed method was tested on a set of light microscopy images of the early development of *Fusarium oxysporum* f.sp. *pisi* and *Alternaria* sp.¹ *Fusarium* [11] and *Alternaria* [12] spp. (*Hyphomycetes*, *Deuteromycotina*)

¹ The specimens were incubated on Czapek-Dox agar at 4 and 20°C and their growth was documented in intervals of approximately 6 and 2 hours, respectively. The images were acquired by a CCD digital camera attached to a conventional light microscope with 100× and 20× magnification, respectively.

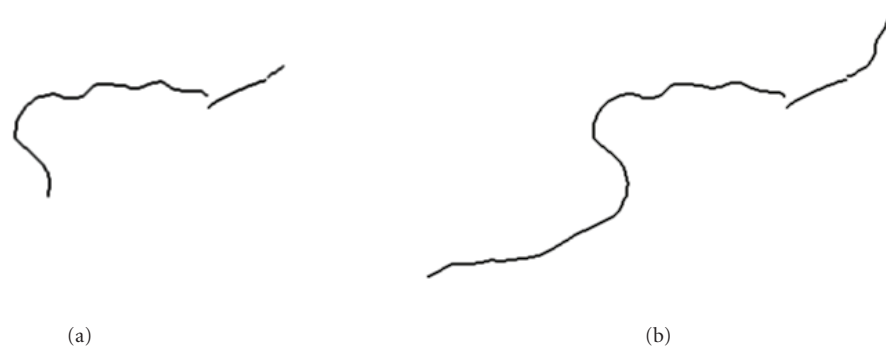


FIGURE 3: Morphological skeletons computed from the segmented images in Figure 2. The separated branches represent the hyphae and the macroconidium.

are phytopathogenic fungi with a worldwide distribution able to cause severe diseases in a wide range of economically important crop plants. Both *Fusarium oxysporum* and *Alternaria* sp. spread by asexual spores, conidia. In proper environmental conditions, particularly temperature and humidity, the conidium germinates by hyphae to form a mycelium. The growth rate of the mycelial colony in optimal conditions is approximately 5–10 mm per day. Detailed understanding of the pathogen development principles could contribute to the increasing efficiency of the disease control.

In the case of processing light microscopy images, several preprocessing steps are necessary to eliminate the degradations introduced during the acquisition process. Light microscopy images often suffer from flat-field, that is, a gradual decrease in brightness from image center to image borders caused by the nonuniformity in illumination of microscopy samples. Flat-field correction consists of estimating the shape of the illumination intensity from a microscopy image acquired without a sample, for example, and adding the deficiency in brightness to the degraded image. As biological specimens are usually thicker than the attainable depth of field, parts of the specimen appear out of focus. In such a case, several images at different focal planes are taken and composed by means of digital multifocal fusion [13] into one image with the whole specimen in focus. Since the microscopic slides with specimens are often replaced manually, rough temporal image registration [7] is necessary to compensate for the resulting shift and rotation between images from different observation sessions. Such displacements can be easily removed by means of a rigid-body transformation. As a result, we obtain roughly aligned, uniformly illuminated microscopy images with the whole specimen in focus (see Figures 1 and 8).

Now we will consider two preprocessed images of one specimen from consecutive observation sessions and describe how they can be utilized to generate images simulating its development over the interval between their acquisitions. First, the specimen is segmented from debris and image background by means of a convenient segmentation method, such as adaptive thresholding. The result is a binary image of the shape of the specimen (see Figure 2). Small ir-

regularities in the shape can be rectified by simple morphological operations, if necessary.

The MS of the specimen is acquired from the segmented image by means of a parallel thinning algorithm described in [14], Section 3. The MS is then divided into branches, that is, linear segments corresponding to nonbranching parts of the filaments (see Figure 3). The positions of the division points are usually selected manually, in the locations of hypha branching or between a conidium and a hypha. The points of branching of the MS can also be computed by means of appropriate morphological operations. We denote the tip of a branch that is connected to other branches as the “fixed end” and the tip from which the growth may continue as the “free end.” As the filaments grow independently, the pairs of corresponding branches are processed separately.

In practice, the second MS does not precisely overlap the whole first MS and the elongation process thus has to be adjusted. A sufficient number of CPs are selected equidistantly along the branch in the second, longer MS from the fixed end towards the free end in the length of the corresponding branch in the first, shorter MS (see Figure 4(a)). The distance between the CPs is, for example, half the average width of the filament. The segment with the CPs is then gradually elongated along the whole branch in the second MS, so that the Euclidean distance between the CPs remains uniform, until it reaches the free end. In this way, we estimate how the CPs were shifting during the missing interval (see Figure 4).

The CPs on the MS computed during the elongation process are replaced for the purpose of image warping by pairs of corresponding CPs on the boundary of the specimen (see Figure 5). These boundary-CPs are situated in the direction perpendicular to the branch in the neighborhood of the corresponding skeleton-CPs so that each skeleton-CP bisects the line segment between the corresponding pair of boundary-CPs. The length of the line segment corresponds to the local thickness of the filament and can be computed as a weighted average of the local thickness in the first and in the second segmented image. In order to preserve the shape of nongrowing round objects, such as conidia, we select a sufficient number of points on their boundary and add them to the set of boundary-CPs (see Figure 9).

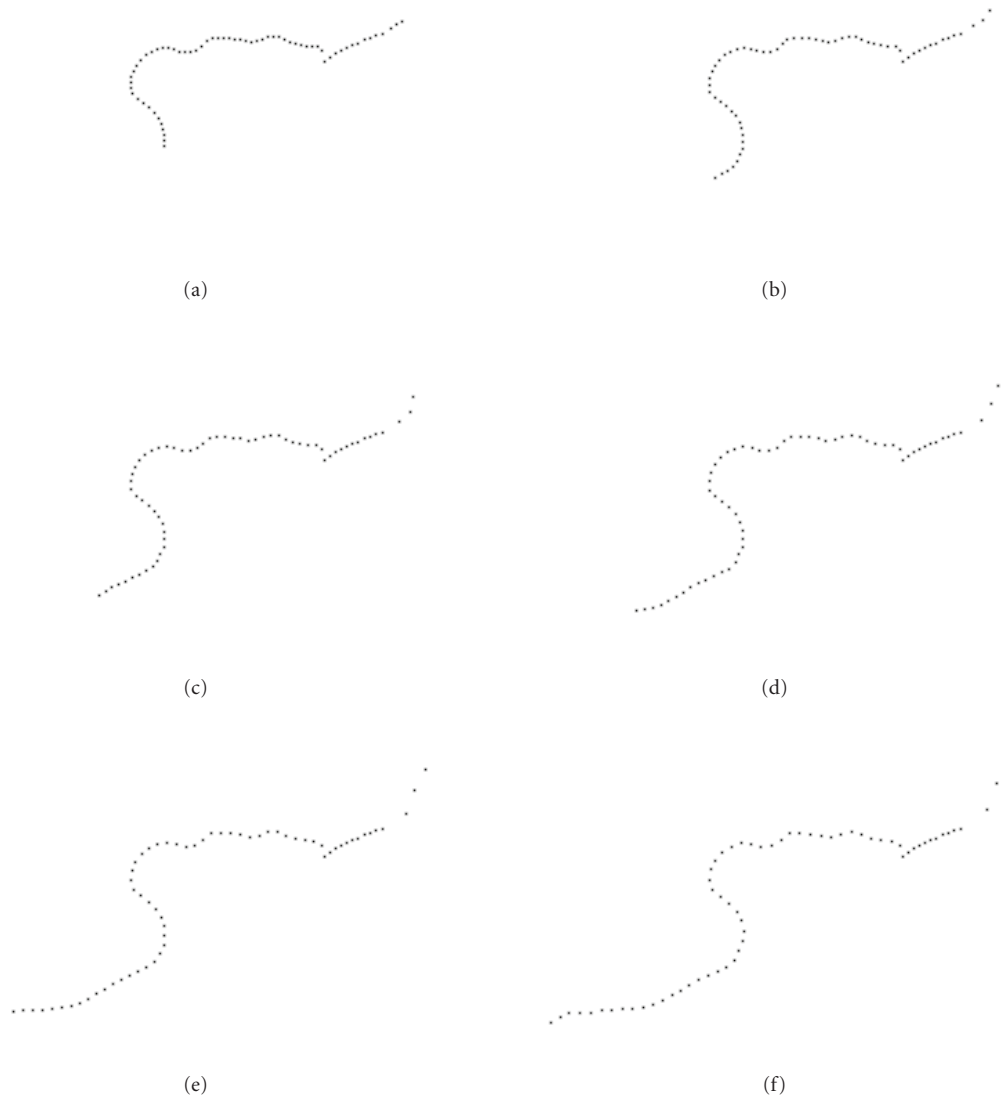


FIGURE 4: (a) Control points selected equidistantly along the branches of the morphological skeleton in Figure 3(b) in the length of the corresponding branches of the morphological skeleton in Figure 3(a). (b)–(f) Stretching of the segments with control points along the morphological skeleton in Figure 3(b). The movement of control points represents the elongation of the hyphae during the examined interval.

Finally, the preprocessed images from the beginning and the end of the missing interval are geometrically transformed by means of thin-plate splines (2). The parameters are defined by the computed boundary-CPs. The transformation maps the boundary-CPs in the input image (see Figure 9(a)) to the corresponding boundary-CPs at an arbitrary instance within the interval (see Figure 9(b)). As the input images are often taken under different conditions, for example, at different focal planes, just the temporally closer image is usually transformed. The warped images, or their weighted combination, represent the specimen at the requested moment between acquisitions. In this way, we can generate a sequence of photorealistic images that show the gradual growth of the specimen over the undocumented interval.

In order to test the performance of the proposed method, we compare an image generated by the process described above with an authentic image acquired for these purposes at the corresponding stage of growth (see Figures 6 and 10). The synthetic image matches the reference image almost perfectly, without significant unnatural deformations (see Figure 7). Such results prove the efficacy of our method.

4. DISCUSSION

The method was designed for images of settled filamentous specimens gradually elongating over time. In the case of nonuniform speed of growth, additional information, for example, images from previous and subsequent observation

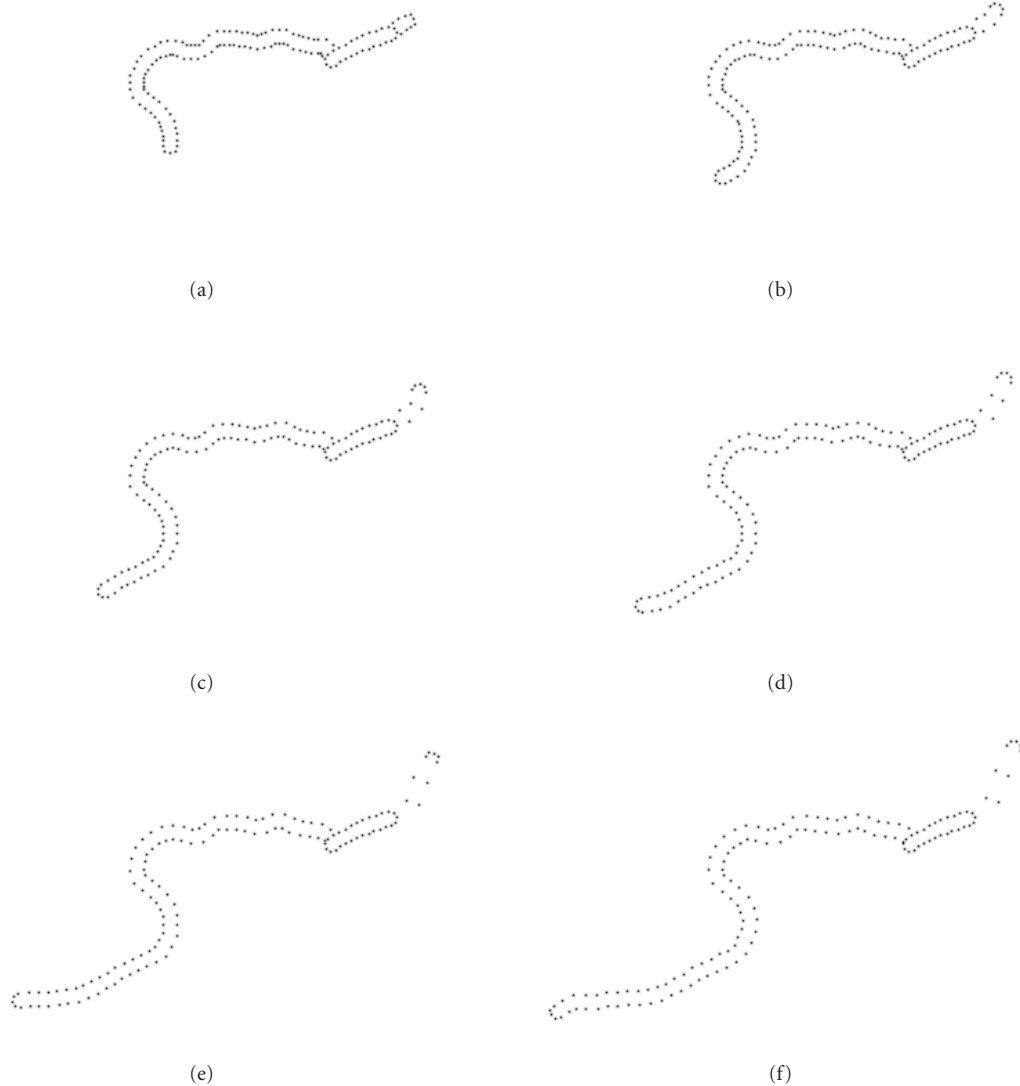


FIGURE 5: Control points on the boundary of the specimen computed from the control points on the morphological skeleton in Figure 4 according to the segmented images in Figure 2. These points on boundary are used as control points in image warping.

sessions, would be necessary to estimate the changes in the speed of elongation of each filament during the examined interval. As only the length of branches is used from the first, earlier MS, the method could be used, to some extent, to generate images of the specimen representing even instances before the acquisition of the first image. This would be limited by the error in estimation of the speed of growth and by the distortion of highly warped images. Small growth in width can be simulated by interpolating the local width of filaments. The apparition of new branches could be partly modeled as well. If the new branch is short enough in one of the acquired images, it is neglected for the purposes of reconstructing the interval before the acquisition whereas in the interval after the acquisition, the branch is processed. Otherwise, we must estimate when the new branch started to develop. Its growth in the interval before its apparition is then

reconstructed by warping just the latter image so that from the beginning of the interval until the estimated moment, the new branch remains as long as the width of the filament. Most of the results, however, suffer from significant deformations. The method can be used for realistic modeling only if the growth consists of stretching and curving of filaments and the already developed parts do not change in shape. If not only elongation but also significant movement is a part of the growth process, a more complex method should be applied. The problem of occlusion, such as overlapping of filaments, has not been satisfactorily solved either. The ability of the proposed method to preserve textures is also limited. If a significant fine texture is present, it may appear deformed in the warped image.

The method allows to generate a series of an arbitrary number of images representing the development of the



FIGURE 6: The specimen at a defined moment within in the interval between observations. The reconstructed image (a) was computed from the image in Figure 1(b) by means of a geometric transformation by thin-plate splines, mapping the control points in Figure 5(f) to their counterparts in Figure 5(d). The reference image (b) was acquired for the purpose of comparison at the corresponding stage of growth. The artificially generated image matches the authentic image almost perfectly, without unnatural deformations.

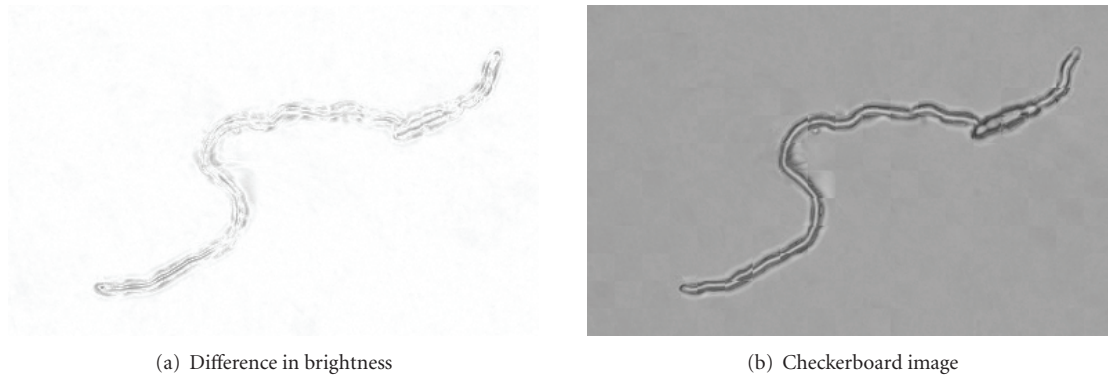


FIGURE 7: Comparison of the artificially generated image in Figure 6(a) and the reference image in Figure 6(b). Synthesized images demonstrating the performance of the proposed method: (a) pixel-wise difference in brightness, (b) a checkerboard image composed of square areas alternately taken from both images.

specimen uniformly over the whole interval. As the interpolation step can be set as small as necessary, the growth can be smoothly visualized as a video sequence. The artificial image should be composed from both warped images only if the geometric transformation is estimated with high accuracy. If the features are not aligned precisely, the combination of two images might produce disturbing double-exposure effects. In such a case, just the temporally closer warped image is taken as the result. The precision can be assured by selecting a sufficient number of CPs. The more CPs are used, the more accurate the mapping function is but the longer the computation of image warping takes. Too short spaces between the CPs could also result in undesired local distortions. The type of the geometric transformation affects the final result as well. Although radial basis functions (1) are formally of a global nature, that is, for every pixel in the image all basis functions ϕ_i ($i = 1, \dots, n$) must be taken into account, they can model local deformations quite well. This depends also on the type of the basis functions ϕ_i used. The thin-plate splines (2) proved efficient for our purposes.

5. CONCLUSIONS

We have introduced a new method for photorealistic modeling of the growth of filamentous specimens in intervals between observations. It was developed for the purpose of completing time studies of settled and relatively slow-growing specimens with filamentous growth patterns, such as fungi and oomycetes. In principle, it can be used to process any objects with such characteristics. The method is based on image warping in combination with growth tracking by means of the morphological skeleton. It can generate realistic images just from the images acquired at the beginning and at the end of the undocumented interval. Furthermore, as the method does not introduce unnatural deformations, it is suitable for biomedical data. Its performance was successfully tested on light microscopy images of *Fusarium oxysporum* and *Alternaria* sp. germination and mycelium growth. The photorealistic appearance of the artificially generated images and high correlation with ground truth proved satisfactory for the purpose of the study.

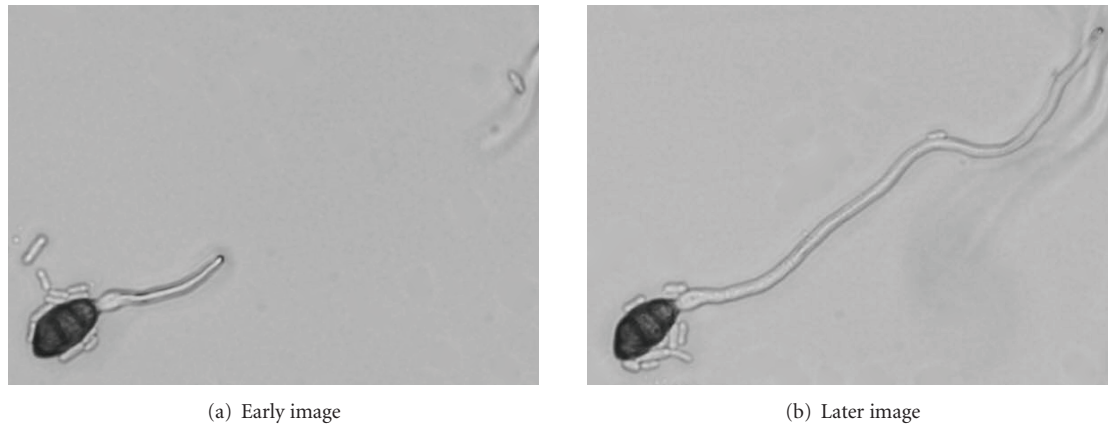


FIGURE 8: *Alternaria* sp. An early (a) and a later (b) image of one specimen from consecutive observation sessions. The development of a hypha from a conidium and its growth in length. Light microscopy images after displacement rectification and debris suppression.

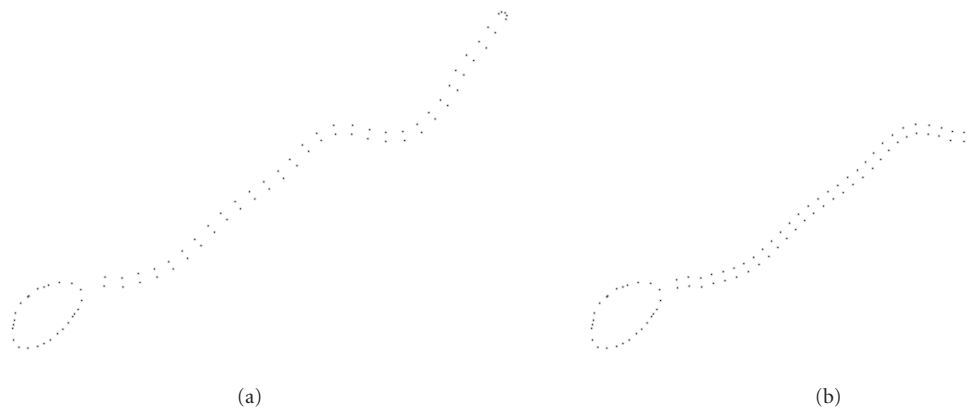


FIGURE 9: Control points on the boundary of the hypha computed during the elongation process plus control points selected on the boundary of the conidium. These points allow us to reconstruct the image of the specimen at $2/3$ of the interval between acquisitions of the images in Figure 8. The image in Figure 8(b) is warped by radial basis functions so that the control points representing the end of the interval (a) are mapped to the corresponding control points at $2/3$ of the interval (b).

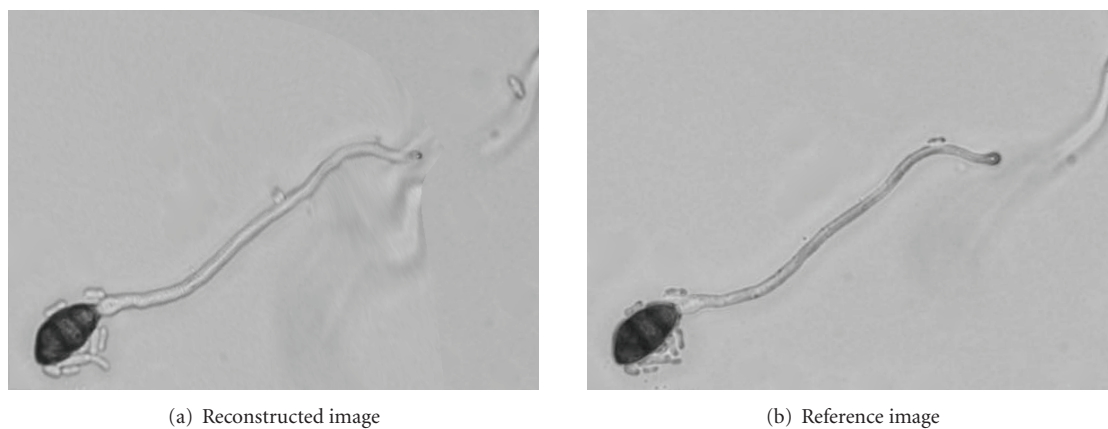


FIGURE 10: The specimen at $2/3$ of the interval between observations. The reconstructed image (a) was computed from the image in Figure 8(b) by means of a geometric transformation by thin-plate splines, mapping the control points in Figure 9(a) to their counterparts in Figure 9(b). The reference image (b) was acquired for the purpose of comparison at the corresponding stage of growth but at a different focal plane, hence the darker texture. Despite this fact, the artificially generated image matches the authentic image very well.

ACKNOWLEDGMENTS

The work has been partly supported by the grant projects GA UK 148207, MŠMT 1M0572, and MSM 6198959215. The fungal strain UPOC-FUN-161 was kindly provided by and its cultivation performed and documented at the Laboratory of Phytopathology, Department of Botany, Faculty of Science, Palacký University (Olomouc, Czech Republic); special acknowledgement to Drahomíra Vondráková.

REFERENCES

- [1] P. Prusinkiewicz, M. Hammel, J. Hanan, and R. Měch, “L-systems: from the theory to visual models of plants,” in *Plants to Ecosystems: Advances in Computational Life Sciences I*, M. T. Michalewicz, Ed., pp. 1–27, CSIRO, Melbourne, Australia, 1996.
- [2] L. Streit, P. Federl, and M. C. Sousa, “Modelling plant variation through growth,” *Computer Graphics Forum*, vol. 24, no. 3, pp. 497–506, 2005.
- [3] J. Schlecht, K. Barnard, E. Spriggs, and B. Pryor, “Inferring grammar-based structure models from 3D microscopy data,” in *Proceedings of the IEEE Computer Society Conference on Computer Vision and Pattern Recognition*, pp. 1–8, Minneapolis, Minn, USA, June 2007.
- [4] G. Wolberg, *Digital Image Warping*, IEEE Computer Society Press, Los Alamitos, Calif, USA, 1990.
- [5] K. Fujimura and M. Makarov, “Foldover-free image warping,” *Graphical Models and Image Processing*, vol. 60, no. 2, pp. 100–111, 1998.
- [6] H. Aboul-Ella and M. Nakajima, “Image metamorphosis transformation of facial images based on elastic body splines,” *Signal Processing*, vol. 70, no. 2, pp. 129–137, 1998.
- [7] B. Zitová and J. Flusser, “Image registration methods: a survey,” *Image and Vision Computing*, vol. 21, no. 11, pp. 977–1000, 2003.
- [8] C. Xu and J. L. Prince, “Generalized gradient vector flow external forces for active contours,” *Signal Processing*, vol. 71, no. 2, pp. 131–139, 1998.
- [9] L. Lam, S.-W. Lee, and C. Y. Suen, “Thinning methodologies – a comprehensive survey,” *IEEE Transactions on Pattern Analysis and Machine Intelligence*, vol. 14, no. 9, pp. 869–885, 1992.
- [10] J. C. Carr, W. R. Fright, and R. K. Beatson, “Surface interpolation with radial basis functions for medical imaging,” *IEEE Transactions on Medical Imaging*, vol. 16, no. 1, pp. 96–107, 1997.
- [11] M. Zemánková and A. Lebeda, “Fusarium species, their taxonomy, variability and significance in plant pathology,” *Plant Protection Science*, vol. 37, pp. 25–42, 2001.
- [12] J. Chelkowski and A. Visconti, Eds., *Alternaria: Biology, Plant Diseases, and Metabolites*, vol. 3 of *Topics in Secondary Metabolism*, Elsevier Science B. V., Amsterdam, The Netherlands, 1992.
- [13] F. Šroubek and J. Flusser, “Fusion of blurred images,” in *Multi-Sensor Image Fusion and Its Applications*, R. S. Blum and Z. Liu, Eds., vol. 26 of *Signal Processing and Communications Series*, pp. 405–430, CRC Press, San Francisco, Calif, USA, 2005.
- [14] Z. Guo and R. W. Hall, “Parallel thinning with two-subiteration algorithms,” *Communications of the ACM*, vol. 32, no. 3, pp. 359–373, 1989.